論文 / 著書情報
Article / Book Information

Title	Superspheres: Intermediate Shapes between Spheres and Polyhedra
Authors	SUSUMU ONAKA
Citation	Polyhedral Structures, Symmetry, and Applications, pp. 121-128
Pub. date	2018, 1

symmetry
MDPI
Article

Superspheres: Intermediate Shapes between Spheres and Polyhedra

Susumu Onaka

Department of Materials Science and Engineering, Tokyo Institute of Technology, 4259-J2-63 Nagatsuta, Yokohama 226-8502, Japan; onaka.s.aa@m.titech.ac.jp; Tel.: +81-45-924-5564; Fax: +81-45-924-5566

Received: 16 May 2012; in revised form: 20 June 2012; Accepted: 25 June 2012; Published: 3 July 2012

Abstract: Using an *x*-*y*-*z* coordinate system, the equations of the superspheres have been extended to describe intermediate shapes between a sphere and various convex polyhedra. Near-polyhedral shapes composed of {100}, {111} and {110} surfaces with round edges are treated in the present study, where {100}, {111} and {110} are the Miller indices of crystals with cubic structures. The three parameters p, a and b are included to describe the {100}-{111}-{110} near-polyhedral shapes, where p describes the degree to which the shape is a polyhedron and a and b determine the ratios of the {100}, {111} and {110} surfaces.

Keywords: supersphere; particle; precipitate; materials science; crystallography

---

1. Introduction

Small crystalline precipitates often form in alloys and have near-polyhedral shapes with round edges. Figure 1 is a transmission electron micrograph showing an example of this where the dark regions, which have shapes between a circle and a square, are Co-Cr alloy particles precipitated in a Cu matrix [1,2]. Why such precipitate shapes form has been explained by the anisotropies of physical properties of metals and alloys originating from the crystal structures [2,3]. Both the Co-Cr alloy particles and Cu matrix have cubic structures. The three-dimensional shapes of the particles shown in Figure 1 are intermediate between a sphere and a cube composed of crystallographic planes {100} as indicated by the Miller indices.

Even if the alloy system such as the Co-Cr alloy particles in the Cu matrix is fixed, the precipitate shapes change as a function of the precipitate size [1,2]. In the case of the Co-Cr alloy precipitates, the spherical to cubical shape transition occurs as the precipitate size increases [2,3]. The size dependence of the precipitate's equilibrium shape determines the shape transitions [2,3]. When we discuss such physical phenomenon, it is convenient to use simple equations that can approximate the precipitate shapes [2–5]. In the present study, we discuss a simple equation that gives shapes intermediate between a sphere and various polyhedra.

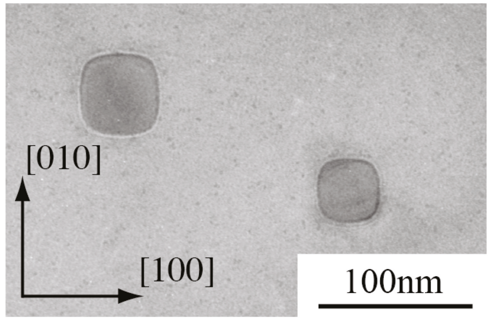

Figure 1. Transmission electron micrograph showing the Co-Cr alloy precipitates in a Cu matrix [1,2].

2. Cubic Superspheres

The solid figure described by

$$|x/R|^p + |y/R|^p + |z/R|^p = 1 \quad (R > 0,\ p \geq 2) \tag{1}$$

expresses a sphere with radius R when $p = 2$ and a cube with edges $2R$ as $p \to \infty$ [2–4]. It is reported in [6] that the 19th century French mathematician Gabriel Lamé first presented this equation. Intermediate shapes between these two limits can be represented by choosing the appropriate value of $p > 2$. In [2–4], such shapes are called superspheres, and Figure 2 shows the shapes given by (1) for (a) $p = 2$, (b) $p = 4$ and (c) $p = 20$. The parameter R determines the size and p determines the polyhedrality, *i.e.*, the degree to which the supersphere is polyhedron. If $|x| > |y|$ and $|x| > |z|$, $|x/R|^p + |y/R|^p + |z/R|^p = 1$ as $p \to \infty$ means $|x/R| = 1$. This describes the limit for (1) as $p \to \infty$ which gives a cube surrounded by three sets of parallel planes, $x = \pm R$, $y = \pm R$ and $z = \pm R$.

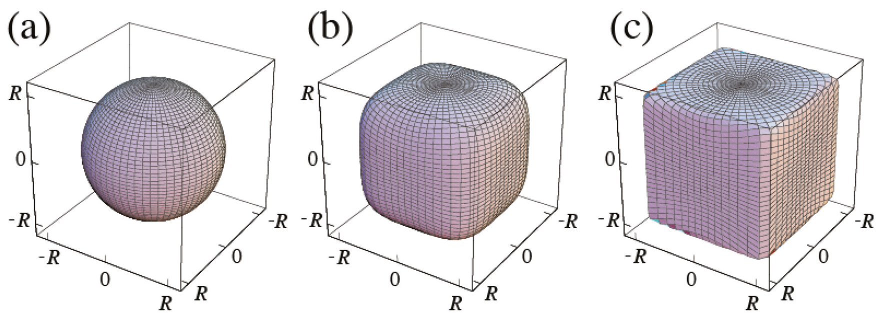

Figure 2. Shapes of the cubic superspheres given by (1); (**a**) $p = 2$; (**b**) $p = 4$ and (**c**) $p = 20$.

3. {111} Regular-Octahedral and {110} Rhombic-Dodecahedral Superspheres

Equation (1) can be rewritten as

$$\left[h_{\text{cube}}(x,y,z)\right]^{1/p} = R \ \text{ where } \ h_{\text{cube}}(x,y,z) = |x|^p + |y|^p + |z|^p \tag{2}$$

This expression has been extended to describe other convex polyhedra [7]. Although the original superspheres discussed in [2–4] are intermediate shapes between a sphere and a cube, now the superspheres can refer to shapes intermediate between various convex polyhedra and a sphere [8].

Superspheres have been used to discuss the shapes of small crystalline particles and precipitates [2, 3,5,8,9]. The planes of crystal facets are indicated by their Miller indices. We use this notation in the present study. The cube given by (2) as $p \to \infty$ is the {100} cube composed of six {100} faces. Assuming crystals with cubic structures, the regular octahedron is the {111} octahedron and the rhombic dodecahedron is the {110} dodecahedron [7].

The {111} octahedral superspheres are given by the following equation:

$$\left[h_{\mathrm{octa}}(x,y,z)\right]^{1/p} = R \tag{3a}$$

where

$$h_{\mathrm{octa}}(x,y,z) = |x+y+z|^p + |-x+y+z|^p + |x-y+z|^p + |x+y-z|^p \tag{3b}$$

The shapes given by (3) are shown in Figure 3.

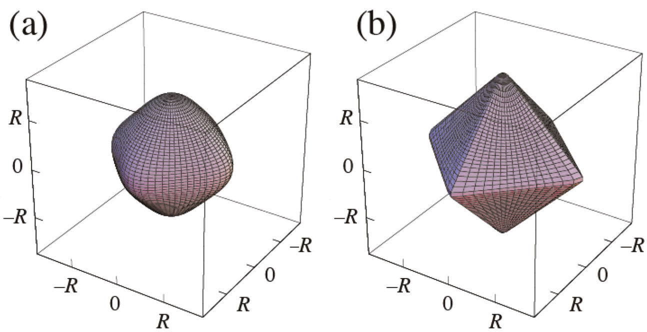

Figure 3. Shapes of the {111} regular-octahedral superspheres given by (3); (**a**) $p = 4$ and (**b**) $p = 40$.

On the other hand, the {110} dodecahedral superspheres are given by

$$\left[h_{\mathrm{dodeca}}(x,y,z)\right]^{1/p} = R \tag{4a}$$

where

$$h_{\mathrm{dodeca}}(x,y,z) = |x+y|^p + |x-y|^p + |y+z|^p + |y-z|^p + |x+z|^p + |x-z|^p \tag{4b}$$

The shapes given by (4) are shown in Figure 4. Equations (2–4) expressed by the spherical coordinate system are shown in [7].

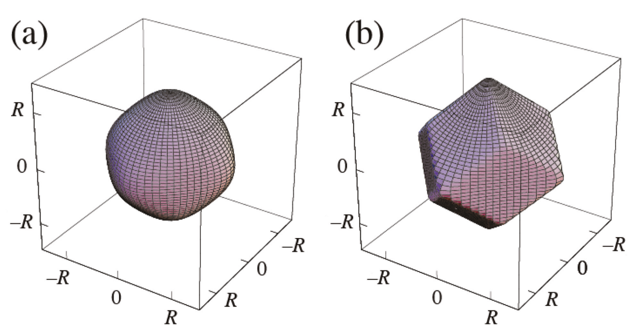

Figure 4. Shapes of the {110} rhombic-dodecahedral superspheres given by (4); (**a**) $p = 6$ and (**b**) $p = 40$.

4. {100}-{111}-{110} Polyhedral Superspheres

Combined superspheres can be expressed by combining the equations of each supersphere. Combining (2), (3) and (4), we get

$$\left[h_{\text{cube}}(x,y,z)+\frac{1}{a^p}h_{\text{octa}}(x,y,z)+\frac{1}{b^p}h_{\text{dodeca}}(x,y,z)\right]^{1/p}=R. \qquad (5)$$

The parameters $a > 0$ and $b > 0$ are those for determining the ratios of the {100}, {110} and {111} surfaces. The shapes of the supersphere given by (5) are shown in Figure 5 when

$$a=\sqrt{3}$$

,

$$b=\sqrt{2}$$

for two values of p.

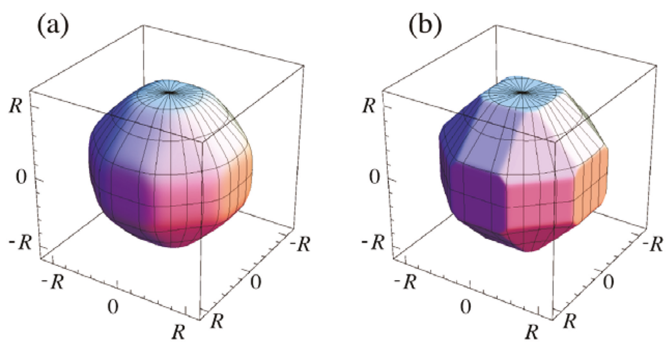

Figure 5. Shapes of the {100}-{111}-{110} polyhedral superspheres given by (5); (**a**) $p = 20$ and (**b**) $p = 100$.

The a and b dependences of the shapes given by (5) are understood by examining the polyhedral shapes as $p \to \infty$. Among the three polyhedra given by $[h_{\text{cube}}(x,y,z)]^{1/p} = R$, $[h_{\text{octa}}(x,y,z)]^{1/p} = aR$ and $[h_{\text{dodeca}}(x,y,z)]^{1/p} = bR$, the innermost surfaces of the polyhedra are retained to form the combined polyhedron. Figure 6 shows the effect of a and b on the shapes given by (5) as $p \to \infty$.The shape is determined by their location in the quadrilateral surrounded by the points P $(a,b) = (3,2)$, Q (2,2), R (1,1) and S (3/2,1). Various shapes in and around the quadrilateral are shown by the insets in Figure 6 can be summarized as follows:

1. Three basic polyhedra

   (a) {100} cube at point P.
   (b) {111} octahedron at point R.
   (c) {110} dodecahedron at point S.

2. Combination of two basic polyhedra

   (a) {100}-{111} polyhedra changing from the {100} cube to the {111} octahedron along the line from P to R via Q, by truncating the eight vertices of the cube (The shape at point Q is {100}-{111} cuboctahedron).

(b) {111}-{110} polyhedra changing from the {111} octahedron to the {110} dodecahedron along the line from R to S, by chamfering the 12 edges of the octahedron.
(c) {110}-{100} polyhedra changing from the {110} dodecahedron to the {100} cube along the line from S to P, by truncating six of the 14 vertices of the dodecahedron.

3. Combinations of all three basic polyhedra

(a) {100}-{111}-{110} polyhedra with mutually non-connected {110} surfaces in Region 1 (R-1).
(b) {100}-{111}-{110} polyhedra with mutually connected {110} surfaces in Region 2 (R-2).

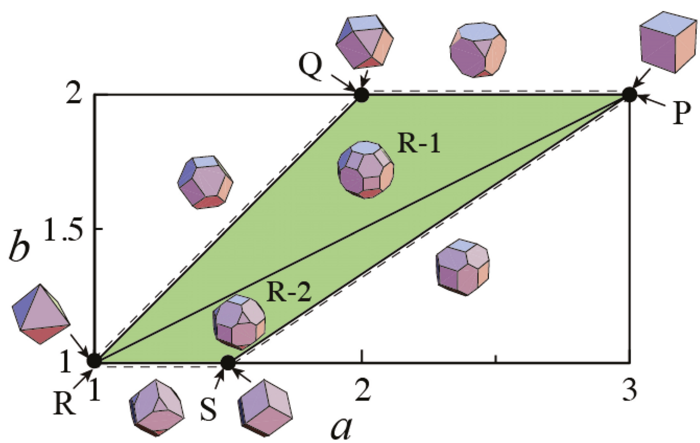

Figure 6. Diagram showing the variation in the shapes of the {100}-{111}-{110} polyhedral superspheres given by (5) as $p \to \infty$.

The boundary between Regions 1 and 2, expressed by the line from P to R, is written as:

$$b = (a+1)/2 \tag{6}$$

Figure 6 is essentially the same as Figure 3 in [7,8] where the parameters $\alpha = 1/a$ and $\beta = 1/b$ are used instead of a and b. In the appendix, the volume and surface area of the polyhedra shown in Figure 6 are written as a function of a and b. The use of the parameters a and b gives a more intuitive diagram (Figure 6), compared with the diagram given by α and β.

5. Discussion

5.1. Shape Transitions of Superspheres from a Sphere to Various Polyhedra

Shape transitions of superspheres from a sphere to a polyhedron are characterized by the change in the normalized surface area $N = S/V^{2/3}$, where S is the surface area and V the volume of the supersphere. For a sphere, $N = 6^{2/3}\pi^{1/3} \approx 4.84$. Figure 7 shows the variations in N as a function of p for the following the superspheres as indicated by the insets:

(i) the {100} cube type given by (2),
(ii) the {111} regular-octahedral type given by (3),
(iii) the {110} rhombic-dodecahedral type given by (4) and
(iv) the {100}-{111}-{110} polyhedral type given by (5) with

$$a = \sqrt{3}$$

and

$$b = \sqrt{2}$$

.

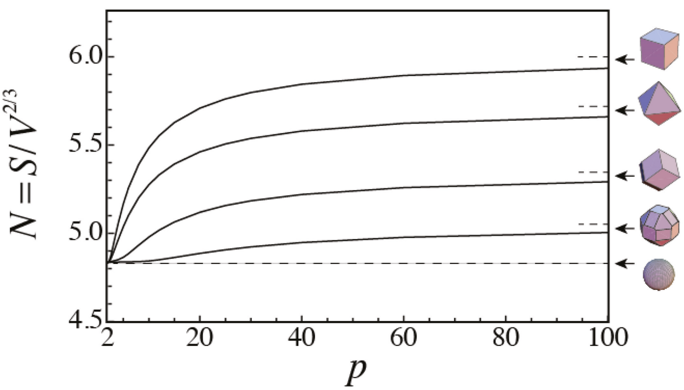

Figure 7. Dependence of the normalized surface area $N = S/V^{2/3}$ on p, where S is the surface area and V the volume for various superspheres: (i) the {100} cube type given by (2); (ii) the {111} octahedral type given by (3); (iii) the {110} dodecahedral type given by (4) and (iv) the {100}-{111}-{110} polyhedral type given by (5) with $a = \sqrt{3}$ and $b = \sqrt{2}$.

The broken lines at the right show the values of N for the polyhedra as $p \to \infty$.

As shown in Figure 7, the change in N with increasing p becomes smaller as the number of faces of polyhedra increases from the {100} cube with 6 to the {100}-{111}-{110} polyhedron with 26. Among the various polyhedra shown in Figure 3, the polyhedron given by

$$a = \sqrt{3}$$

and

$$b = \sqrt{2}$$

in Region 1 with $N = S/V^{2/3} \approx 5.05$ has the minimum total surface area S for the same V [8,10]. The a and b dependence of N can be calculated easily using the results shown in the appendix.

5.2. *Shape of Small Metal Particles*

The shapes of small metal particles observed in previous studies have been discussed previously using the superspherical approximation [8]. Menon and Martin reported the production of ultrafine Ni particles by vapor condensation in an inert gas plasma reactor [11]. They have also reported the crystallographic characterization of these particles by transmission electron microscopy [11]. Near-polyhedral shapes of nanoparticles have been observed to discuss their properties [12–15]. The superspherical approximation is a useful geometrical tool to describe the near-polyhedral shapes.

Acknowledgments: This research was supported by a Grand-in-Aid for Scientific Research C (22560657) by the Japan Society for the Promotion of Science.

appendix

6.

The volume and surface area of the polyhedra shown in Figure 3.

The volume $V$and the {100}, {111} and {110}

surface area, S_{100}, S_{111} and S_{110} of the polyhedra shown in Figure 6 are written as a function of a and b. In Region 1, these are given by

$$V = 4\left[\frac{a^3}{3} - (a-1)^3 - (a-b)^2(6-a-2b)\right]R^3 \tag{A1}$$

$$S_{100} = 12\left[(a-1)^2 - 2(a-b)^2\right]R^2 \tag{A2}$$

$$S_{111} = 4\sqrt{3}\left[(3-a)^2 - 3(2-b)^2\right]R^2 \tag{A3}$$

and

$$S_{110} = 24\sqrt{2}(a-b)(2-b)R^2 \tag{A4}$$

In Region 2, these are

$$V = 2\left[b^3 - \frac{1}{3}(3b-2a)^3 - 4(b-1)^3\right]R^3 \tag{A5}$$

$$S_{100} = 24(b-1)^2 R^2 \tag{A6}$$

$$S_{111} = 4\sqrt{3}(3b-2a)^2 R^2 \tag{A7}$$

and

$$S_{110} = 6\sqrt{2}\left[b^2 - (3b-2a)^2 - 4(b-1)^2\right]R^2 \tag{A8}$$

when $a = 1$ and $b = 1$, the shape given by (5) as $p \to \infty$ is the {111} regular-octahedron as shown by Figure 6. Since the {111} regular-octahedron belongs to both Regions 1 and 2, from both (A1) to (A4) and (A5) to (A8), we get $V = (4/3)R^3$, $S_{100} = 0$, $S_{111} = 4\sqrt{3}R^2$ and $S_{110} = 0$ as it should be.

References

1. Fujii, T.; Tamura, T.; Kato, M.; Onaka, S. Size-Dependent equilibrium shape of Co-Cr particles in Cu. *Microsc. Microanal.* **2002**, *8*, 1434–1435.
2. Onaka, S.; Kobayashi, N.; Fujii, T.; Kato, M. Energy analysis with a superspherical shape approximation on the spherical to cubical shape transitions of coherent precipitates in cubic materials. *Mat. Sci. Eng.* **2002**, *A347*, 42–49.
3. Onaka, S.; Kobayashi, N.; Fujii, T.; Kato, M. Simplified energy analysis on the equilibrium shape of coherent γ' precipitates in gamma matrix with a superspherical shape approximation. *Intermetallics* **2002**, *10*, 343–346. [CrossRef]
4. Onaka, S. Averaged Eshelby tensor and elastic strain energy of a superspherical inclusion with uniform eigenstrains. *Phil. Mag. Let.* **2001**, *81*, 265–272. [CrossRef]
5. Onaka, S. Geometrical analysis of near polyhedral shapes with round edges in small crystalline particles or precipitates. *J. Mat. Sci.* **2008**, *43*, 2680–2685. [CrossRef]
6. Jaklic, A.; Leonardis, A.; Solina, F. *Segmentation and Recovery of Superquadrics (Computational Imaging and Vision)*; Kluwer Academic: Dordrecht, The Netherlands, 2000; Volume 20, pp. 13–39.

7. Onaka, S. Simple equations giving shapes of various convex polyhedra: The regular polyhedra and polyhedra composed of crystallographically low-index planes. *Phil. Mag. Let.* **2006**, *86*, 175–183. [CrossRef]
8. Miyazawa, T.; Aratake, M.; Onaka, S. Superspherical-shape approximation to describe the morphology of small crystalline particles having near-polyhedral shapes with round edges. *J. Math. Chem.* **2012**, *50*, 249–260. [CrossRef]
9. Onaka, S.; Fujii, T.; Kato, M. Elastic strain energy due to misfit strains in a polyhedral precipitate composed of low-index planes. *Acta Mater.* **2007**, *55*, 669–673. [CrossRef]
10. Suárez, J.; Gancedo, E.; Manuel Álvarez, J.; Morán, A. Optimum compactness structures derived from the regular octahedron. *Eng. Struct.* **2008**, *30*, 3396–3398. [CrossRef]
11. Menon, S.K.; Martin, P.L. Determination of the anisotropy of surface free energy of fine metal particles. *Ultramicroscopy* **1986**, *20*, 93–98. [CrossRef]
12. Wang, G.L. Transmission electron microscopy of shape-controlled nanocrystals and their assemblies. *J. Phys. Chem.* **2000**, *104*, 1153–1175. [CrossRef]
13. Niu, W.; Zheng, S.; Wang, D.; Liu, X.; Li, H.; Han, S.; Chen, J.; Tang, Z.; Xu, G. Selective synthesis of single-crystalline rhombic dodecahedral, octahedral, and cubic gold nanocrystals. *J. Am. Chem. Soc.* **2009**, *131*, 697–703.
14. Jeong, G.W.; Kim, M.; Lee, Y.W.; Choi, W.; Oh, W.T.; Park, Q.-H.; Han, S.W. Polyhedral Au Nanocrystals exclusively bound by {110} facts: The rhombic dodecahedron. *J. Am. Chem. Soc.* **2009**, *131*, 1672–1673.
15. Ribis, J.; de Carlan, Y. Interfacial strained structure and orientation relationships of the nanosized oxide particles deduced from elasticity-driven morphology in oxide dispersion strengthened materials. *Acta Mater.* **2012**, *60*, 238–252. [CrossRef]